

The inner engine of GeV-radiation-emitting gamma-ray bursts

R. Ruffini,^{1,2} J. A. Rueda,^{1,2} R. Moradi,^{1,2} Y. Wang,^{1,2} S. S. Xue^{1,2} L. Becerra,^{1,3}
 C. L. Bianco,^{1,2} Y. C. Chen,^{1,2} C. Cherubini,^{4,5} S. Filippi,^{4,5} M. Karlica,^{1,2}
 J. D. Melon Fuksman,^{1,2} D. Primorac,^{1,2} N. Sahakyan,^{1,6} G. V. Vereshchagin,^{1,2}

¹*International Center for Relativistic Astrophysics Network,
 Piazza della Repubblica 10, I-65122 Pescara, Italy*

²*ICRA and Dipartimento di Fisica, Università di Roma "La Sapienza", Piazzale Aldo Moro 5, I-00185 Roma, Italy*

³*Escuela de Física, Universidad Industrial de Santander, A.A.678, Bucaramanga, 680002, Colombia*

⁴*Department of Engineering, University Campus Bio-Medico of Rome,
 Nonlinear Physics and Mathematical Modeling Lab, Via Alvaro del Portillo 21, 00128 Rome, Italy*

⁵*International Center for Relativistic Astrophysics ICRA,*

University Campus Bio-Medico of Rome, Via Alvaro del Portillo 21, I-00128 Rome, Italy

⁶*ICRANet-Armenia, Marshall Baghramian Avenue 24a, Yerevan 0019, Armenia.*

(Dated: May 21, 2022)

We motivate how the most recent progress in the understanding the nature of the GeV radiation in most energetic gamma-ray bursts (GRBs), the binary-driven hypernovae (BdHNe), has led to the solution of a forty years unsolved problem in relativistic astrophysics: how to extract the rotational energy from a Kerr black hole for powering synchrotron emission and ultra high-energy cosmic rays. The *inner engine* is identified in the proper use of a classical solution introduced by Wald in 1972 duly extended to the most extreme conditions found around the newly-born black hole in a BdHN. The energy extraction process occurs in a sequence impulsive processes each accelerating protons to 10^{21} eV in a timescale of 10^{-6} s and in presence of an external magnetic field of 10^{13} G. Specific example is given for a black hole of initial angular momentum $J = 0.3 M^2$ and mass $M \approx 3 M_{\odot}$ leading to the GeV radiation of 10^{49} erg·s⁻¹. The process can energetically continue for thousands of years.

INTRODUCTION

The understanding of gamma-ray bursts (GRBs), ongoing since almost fifty years, has been recently modified by the introduction of eight different subclasses of GRBs with binary progenitors composed of different combinations of neutron stars (NSs), carbon-oxygen cores (CO_{core}) leading to supernovae (SNe), white dwarfs (WDs), and black holes (BHs), here indicated as Papers I.1 [1–3]. This approach contrast with the traditional ones which assume all GRBs originating from a single BH with an ultra-relativistic jet extending from the prompt-emission phase (PEP) all the way to the late observable GRB phases. Special attention has been given to identify the different components of a special class of GRBs originating from a tight binary system, of orbital period ~ 5 min, composed of a CO_{core}, undergoing a SN event, and a NS companion. We have called these systems binary-driven hypernovae (BdHNe). In particular, in Papers I.2 [4–8] we have studied the physics of the hypercritical accretion of the SN ejecta onto the companion NS, and in Papers I.3 [7, 9] we have visualized by three-dimensional (3D) smoothed-particle-hydrodynamics (SPH) simulations the process of BH formation (see Fig. 1). From these works it has been clearly evidenced that the BH formation does not occur, as often idealized, in an asymptotically flat empty space but, it is surrounded by plasma undergoing quantum and classic ultra-relativistic regimes.

In 2018, we have further evidenced in Paper II.1 [10]

that in the GRB, itself a BdHN, the PEP, originating from the self-accelerating electron-positron (e^-e^+) plasma reaching Lorentz factor $\Gamma \sim 500$, is constituted by two spikes separated by ~ 20 s. Moreover, the impact of such a PEP on the SN ejecta gives origin to the gamma-ray flares and to the X-ray flares, and to an extended X-ray emission (EXE). Such an EXE occurs during the acceleration phase from the SN ejecta into a hypernova (HN). All these components have $\Gamma \lesssim 4$. In Paper II.2 [11] we have given the basis for the model independent determination of the Lorentz factor $\Gamma \lesssim 2$ in the X-ray flares during the GRB plateau phase with explicit computation performed on 16 BdHNe. In Paper II.3 [12] we developed an afterglow description consistent with a mildly-relativistic expansion for the afterglow of GRB 130427A. There we have also evidenced the specific role of the pulsar-like behaviour of the ν NS, originated from the SN explosion of the CO_{core} and fitted the observed synchrotron emission spectra of the afterglow within a mildly-relativistic expansion with $\Gamma \sim 2$.

From the above, it clearly follows that the traditional approach of assuming a single ultrarelativistic phase extending from the PEP to the late GeV-emission phase (GeV-P) is untenable. The strong limit imposed by the mildly-relativistic expansion of the plateau and afterglow phase request an alternative approach to the GeV-P alternative to the currently accepted one. In Paper III.1 [13] we have evidenced that the transparency condition of the GeV-P imposes the presence of Lorentz factor $\Gamma \sim 1500$ in the emission of the GeV radiation occur-

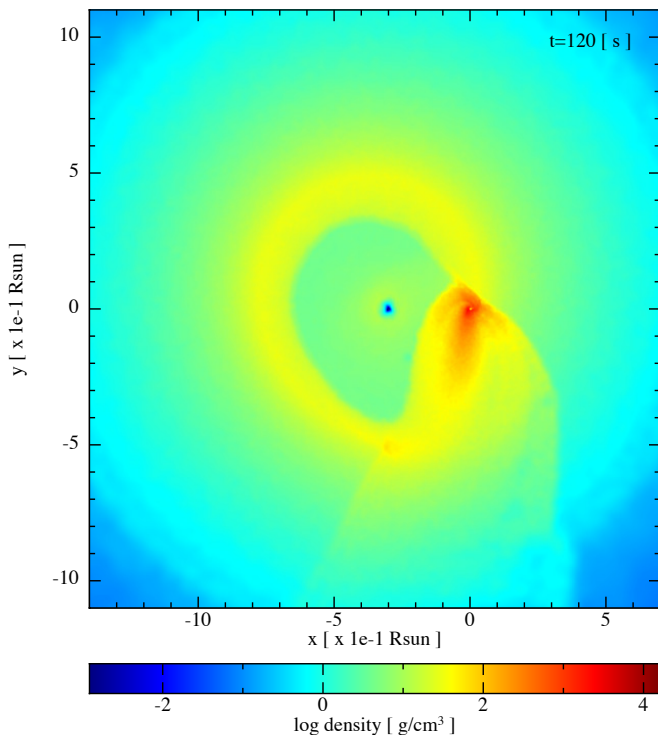


Figure 1. Selected SPH simulations from [9] of the exploding CO_{core} as SN in presence of a companion NS: Model ‘25m1p08e’ with $P_{\text{orb}} = 4.8$ min. The CO_{core} is taken from the $25 M_{\odot}$ zero-age main-sequence (ZAMS) progenitor, so it has a mass $M_{\text{CO}} = 6.85 M_{\odot}$. The mass of the NS companion is $M_{\text{NS}} = 2 M_{\odot}$. It is shown the density profile on the equatorial plane; the coordinate system has been rotated and translated in such a way that the NS companion is at the origin and the νNS is along the $-x$ axis. The snapshot is at the time of the gravitational collapse of the NS companion to a BH, $t = 120$ s from the SN shock breakout ($t = 0$ of our simulation). The system forms a new binary system composed by the νNS (at the center of the deep-blue region) and the BH formed by the collapse of the NS companion (at the center of the red vortices). The SN ejecta is the ionized medium that supplies the BH with the charged particles needed for the realization of the elementary processes leading to the Wald’s solution.

ring at radii of the $\sim 10^{17}$ cm. We have also shown there the existence a correlation between the total energy in e^+e^- plasma in the PEP and the total energy emitted by the GeV-P (see Fig. 7 in Paper III.1).

These factors have motivated our decision to solve both the origin of the PEP and GeV-P with a new energy source using the BH physics. We have shown in that paper a first result: that the rotational energy of a Kerr BH is sufficient to explain the entire GeV-P. From this result, in turn, we have determine the mass and the spin of the BH using the data of the observed GeV luminosity of 21 BdHNe. Using energy conservation argument, we have determined the slowing down rate of the Kerr BH.

Specifically for GRB 130427A we have obtained

$$a = 0.3 M, \quad M = 2.28 M_{\odot}, \quad (1)$$

which lead to a luminosity of $\sim 10^{50}$ erg s^{-1} and (see Tables 5 and 8 in Paper III.1 for details). Here M and $a = J/M$ are the total mass and specific angular momentum of the Kerr BH, being J its angular momentum.

For obtaining these results we used the mass-energy formula of the Kerr BH, Christodoulou [14], and the one of the Kerr-Newman BH, Christodoulou and Ruffini [15] and Hawking [16], Hawking [17],

$$M^2 = \frac{J^2}{4M_{\text{irr}}^2} + \left(\frac{Q^2}{4M_{\text{irr}}} + M_{\text{irr}} \right)^2, \quad (2.1)$$

$$S = 16\pi M_{\text{irr}}^2, \quad (2.2)$$

$$\delta S = 32\pi M_{\text{irr}} \delta M_{\text{irr}} \geq 0, \quad (2.3)$$

where Q and M_{irr} and S are the charge, irreducible mass and horizon surface area of the BH (in $c = G = 1$ units).

We turn now here, first to the physical quantum and classical electrodynamics relativistic model able to explain the luminosity and spectra of the observed GeV-P as well as the creation of the e^+e^- plasma of the PEP by vacuum polarization process, in terms of the rotational energy of the Kerr BH and attempt as well to direct attention to explain the origin of ultra high-energy cosmic rays.

We now assume that the *central engine* of the GRB originates in the electro-dynamical properties of a Papapetrou-Wald-Gibbons field [18–20] which occurs when “a stationary axisymmetric black hole which is placed in an originally uniform magnetic (test) field of strength B_0 aligned along the axis of symmetry of the black hole” [19]. The field B_0 is assumed to be constant in time.

We assume this *central engine* be surrounded by 1) an ionized plasma here, composed for simplicity, by protons and electrons, although the results can be easily generalized to the case of ions. 2) The external sources of magnetic field B_0 originated from e.g. by the pulsar-like or multipole, e.g. toroidal, magnetic field of the νNS [12, 21], or by the fossil field of the collapsed NS that led to the BH. In either case, such sources should be located within a radius $R = 1/B_0$, in order to avoid unnecessary complications [22]. 3) The HN ejecta in the equatorial plane of the binary progenitor (see e.g. Fig. 1, also Fig. 1 in paper II.1 and Refs. [7, 9]). This ionized medium supply the BH with the charged particles needed to establish the elementary process that lead to the Wald’s solution.

The Kerr space-time metric (geometric units will be considered), which is stationary and axisymmetric, in

standard Boyer-Lindquist (BL) coordinates reads [23]

$$ds^2 = - \left(1 - \frac{2Mr}{\Sigma} \right) dt^2 - \frac{4aMr \sin^2 \theta}{\Sigma} dt d\phi + \frac{\Sigma}{\Delta} dr^2 + \Sigma d\theta^2 + \left[r^2 + a^2 + \frac{2Mra^2 \sin^2 \theta}{\Sigma} \right] \sin^2 \theta d\phi^2, \quad (3)$$

where $\Sigma = r^2 + a^2 \cos^2 \theta$ and $\Delta = r^2 - 2Mr + a^2$. The (outer) event horizon is located at $r_+ = M + \sqrt{M^2 - a^2}$.

The electromagnetic field of the *central engine* in orthonormal tetrad is:

$$E_{\hat{r}} = \frac{aB_0}{\Sigma} \left(r \sin^2 \theta - \frac{M (\cos^2 \theta + 1) (r^2 - a^2 \cos^2 \theta)}{\Sigma} \right), \quad (4)$$

$$E_{\hat{\theta}} = \frac{aB_0}{\Sigma} \sin \theta \cos \theta \sqrt{\Delta}, \quad (5)$$

$$B_{\hat{r}} = - \frac{B_0 \cos \theta \left(-\frac{2a^2 Mr (\cos^2 \theta + 1)}{\Sigma} + a^2 + r^2 \right)}{\Sigma}, \quad (6)$$

$$B_{\hat{\theta}} = \frac{B_0 r}{\Sigma} \sin \theta \sqrt{\Delta}. \quad (7)$$

The most complex case of $\theta \neq 0$ will be considered elsewhere, we here for simplicity evaluate the field in the polar direction $\theta = 0$:

$$E_{\hat{r}} = -B_0 \frac{2J (r^2 - a^2)}{(r^2 + a^2)^2} \quad (8)$$

$$E_{\hat{\theta}} = 0 \quad (9)$$

$$B_{\hat{r}} = \frac{B_0 \left(-\frac{4Jar}{(r^2 + a^2)} + a^2 + r^2 \right)}{(r^2 + a^2)} \quad (10)$$

$$B_{\hat{\theta}} = 0. \quad (11)$$

In order to evaluate more simply the energetics of the *central engine* we introduce instead of Eq. (8) the new equation which, for the specific case of our GRBs, facilitates the comprehension of the nature of the *inner engine*

$$E_{\hat{r}} \approx - \frac{B_0 J r_+^2}{2M^2 r^2}. \quad (12)$$

In particular, Eq. (12) allows to introduce only for the sake of a quantitative estimation, the *effective charge*

$$Q_{\text{eff}} = \frac{B_0 J}{2M^2} r_+^2. \quad (13)$$

The two equations (8) and (12) are in an excellent agreement, see Fig. 2, and lead to indistinguishable quantitative results in the case of 21 GRBs considered in Paper III.1. Equation (12) allows a more direct and straightforward evaluation of the leading terms. In the case $\theta \neq 0$ a multipolar distribution of charges should be considered.

Far from imposing any stationarity condition as often adopted in literature we examine a strongly time varying

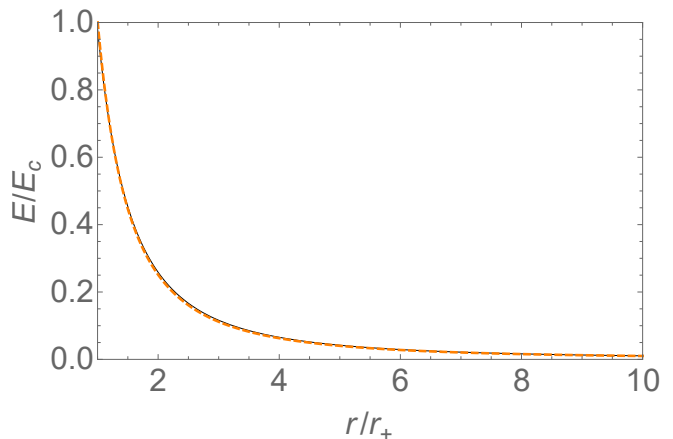


Figure 2. Comparison of electric field given by the full expression (solid-black curve) given by Eq. (8) with the approximate expression (dashed-orange curve) given by Eq. (12). Here we have used for the sake of example $a = 0.3M$ and $B_0/B_c \approx 6.7$, where $B_c = E_c$ being E_c the critical field (14). The parameters a and B_0 are such that the radial electric field at the horizon equals E_c . The quantitative relative difference between Eqs. (8) and (12) in this range of r/r_+ is only 2–4%.

solution composed of a very large number of *impulsive emissions*. Each one of this *impulsive emissions*, originate, in presence of an magnetized and ionized plasma, from the discharge of an electric field E with

$$E \lesssim E_c = \frac{m_e c^3}{e \hbar}, \quad (14)$$

where E_c is the critical field, with m_e and e the electron mass and charge, respectively.

We assume that the magnetic field and the spin of the BH are antiparallel: protons in the surrounding ionized circumburst medium will be repelled, while electrons will be pulled in the BH.

Each impulsive event leads to a small loss of the rotational energy of the BH. All the attention of this Letter is directed to understand the physics of the initial, single elementary impulsive emission where protons will be accelerated to the energy of the 10^{21} eV. The sequence of *impulsive emissions* is simply reconstructed by an iterative process which takes into due account the loss of the rotational energy at the end of each impulse.

The general, qualitative and quantitative features of the system can be obtained from a simple analysis and are as follows:

1) The rotating Kerr BH and the external uniform magnetic field B_0 induce an electric potential leading to a field near the horizon

$$\begin{aligned} E_{r_+} &\approx \frac{JB_0}{2M^2} = \frac{Q_{\text{eff}}}{r_+^2} = \Omega_+ r_+ B_0 \\ &= 6.5 \times 10^{15} \cdot \xi \beta \frac{\text{V}}{\text{cm}}, \end{aligned} \quad (15)$$

where $\xi \equiv a/M = J/M^2$ and $\beta \equiv B_0/B_c$, $B_c = E_c$ where E_c is the critical field (14) and $\Omega_+ = a/(r_+^2 + a^2) = a/(2Mr_+)$.

2) The associated electric potential difference,

$$\begin{aligned} \Delta\phi &= \frac{\epsilon_p}{e} = \int_{r_+}^{\infty} E dr = E_{r_+} r_+ \\ &= 9.7 \times 10^{20} \cdot \xi \beta \mu (1 + \sqrt{1 - \xi^2}) \frac{V}{e}, \end{aligned} \quad (16)$$

where $\mu \equiv M/M_\odot$, accelerates protons along the symmetry axis to Lorentz factors $\gamma_p = e\Delta\phi/(m_p c^2) \sim 10^{12}$, so to energies $\epsilon_p = \gamma_p m_p c^2 \sim 10^{21}$ eV.

3) For $\theta \neq 0$ the protons interact with the dense circumburst medium of the SN ejecta (see Fig. 1), reaching lower values of γ_p , e.g. via synchrotron process, leading to photons of energies ϵ_γ in the observed GeV range.

4) The electrostatic energy available to accelerate protons is

$$\mathcal{E} = \frac{1}{2} E_{r_+}^2 r_+^3 \approx 7.5 \times 10^{41} \cdot \xi^2 \beta^2 \mu^3 (1 + \sqrt{1 - \xi^2})^3 \quad \text{erg}, \quad (17)$$

from which we can infer a number of protons

$$N_p = \frac{\mathcal{E}}{\epsilon_p} \approx 4.8 \times 10^{32} \xi \beta \mu^2 (1 + \sqrt{1 - \xi^2})^2. \quad (18)$$

5) The timescale of the elementary process is given by the time needed to accelerate the protons, i.e.

$$\Delta t_{\text{el}} = \frac{\Delta\phi}{E_{r_+} c} = \frac{r_+}{c} \approx 4.9 \times 10^{-6} \mu (1 + \sqrt{1 - \xi^2}) \quad \text{s}. \quad (19)$$

6) Therefore, the electric power of the system is

$$\dot{\mathcal{E}} \approx \frac{\mathcal{E}}{\Delta t_{\text{el}}} = 1.5 \times 10^{47} \cdot \xi^2 \beta^2 \mu^2 (1 + \sqrt{1 - \xi^2})^2 \quad \text{erg} \cdot \text{s}^{-1}, \quad (20)$$

For example, in the case $\mu \approx 2.3$, $\xi = 0.3$, see Eq. (1), and an electric field at the horizon equal to the critical field, which is obtained for $\beta = 2/\xi \approx 6.7$ (see Eq. 15), we obtain $N_p \approx 1.94 \times 10^{34}$ protons and $\dot{\mathcal{E}} \approx 1.2 \times 10^{49}$ erg s⁻¹. This is in an excellent agreement with the GeV luminosity of the BdHN GRB 130427A after the prompt emission (see Paper III.1 for details). This means that the system, at every time interval Δt_{el} , has to fully shield the induced electric field (15). This is guaranteed by the circumburst, ionized medium (see Fig. 1) which supplies the protons that are accelerated outward and the electrons that fall to the BH.

In the elementary process timescale the BH experiences a fractional change of angular momentum

$$\frac{|\Delta J|}{J} = \frac{|\dot{J}|}{J} \Delta t_{\text{el}} \sim \frac{|\Delta M|}{M} = \frac{|\dot{M}|}{M} \Delta t_{\text{el}}, \quad (21)$$

which, using that the BH mass changes by $|\dot{M}| \approx L_{\text{GeV}}$ (see Paper III.1), where L_{GeV} is the observed GeV luminosity, and using the same numbers we used above

($L_{\text{GeV}} = 10^{49}$ erg s⁻¹), leads to $|\Delta J|/J \approx 10^{-10}$. Then, the system starts over with a new elementary process, inducing a new electric field (15) now given by the new values of $J = J_0 - \Delta J$ and $M = M_0 - \Delta M$ and with B unchanged since the field is external.

The negative charges absorbed by the *inner engine* will lead to the Wald solution with zero electrostatic energy so allowing the system to start again for a new single impulsive event.

The protons outside the symmetry axis experience energy losses, e.g. synchrotron emission. The proton Lorentz factor is limited by synchrotron losses to a value set by the equilibrium between energy gain and energy loss per unit time, i.e. $\dot{E}_{\text{gain}} = \dot{E}_{\text{loss}}$, where

$$\dot{E}_{\text{gain}} = \frac{e B_0 c}{2\pi}, \quad \dot{E}_{\text{loss}} = \frac{2}{3} \frac{e^4 B_0^2 \gamma_{\text{max,p}}^2}{m_p^2 c^3}, \quad (22)$$

which lead to a maximum proton Lorentz factor

$$\gamma_{\text{max,p}} = \left(\frac{3}{4\pi\alpha} \right)^{1/2} \left(\frac{m_p}{m_e} \right)^{1/2} \frac{1}{\beta^{1/2}} \approx \frac{1.05 \times 10^4}{\beta^{1/2}}, \quad (23)$$

and, consequently, to a maximum energy of the proton-synchrotron photons

$$\epsilon_{\text{max},\gamma} = \frac{e\hbar}{m_p c} B_0 \gamma_{\text{max,p}}^2 = \frac{3}{4\pi} \frac{m_p c^2}{\alpha} \approx 30.7 \text{ GeV}. \quad (24)$$

where α is the fine structure constant.

The proton-synchrotron luminosity is therefore

$$\dot{E}_{\text{loss}} \approx 6.4 \times 10^{14} \beta \quad \text{erg} \cdot \text{s}^{-1}. \quad (25)$$

For the example numbers given above, see Eq. (1) and $\beta \approx 6.7$, $\dot{E}_{\text{loss}} \approx 4.3 \times 10^{15}$ erg s⁻¹. From this we infer that, in order to obtain a luminosity of GeV photons of the order of few 10^{49} erg s⁻¹, we would need 10^{34} protons. This number of protons is in full agreement with the available protons in the elementary process, as we have determined from the energy budget. The analysis of this sequence is performed in a complementary work [24] and exemplified in the case of GRB 130427A. There, we first show from the observed GeV emission that the timescale of the elementary process increases with time following a precise linear law with time, i.e. the process becomes less efficient with time. Second, we show that this increasing timescale is explained by the evolution/decrease of the particle density of the HN ejecta around the BH site. The fit of the GeV emission observed and the expected ultra high-energy cosmic rays in the 21 BdHNe in Paper III.1 is under computation and will be presented elsewhere.

We would like to stress that Eq. (12) has been chosen only for mathematical and physical convenience to evaluate the leading orders with excellent approximation. However, the two equations remain conceptually

very different. Equation Eq. (12) can lead to an *effective charge* interpretation of the phenomenon, but Eq. (8) corresponds to the real physical nature of the *inner engine*. The two approaches quantitatively in an excellent approximation coincide but that small difference in Fig. 2 is therefore crucial in differentiating the two conceptually very different physical processes. This can have paramount importance in the understanding of similarly fundamental physics issues.

Before concluding, we would like to mention that the relevance of the Wald's solution has been recently evidenced in the context of NS-BH mergers Levin et al. [25]. They have shown that the dipole field of the NS at the BH horizon position can lead to an electromagnetic emission of interest in the approach to merger when the binary separation distance is very small and therefore the magnetic field at the BH site increases. This scenario involves a much less energetic situation that could be relevant for precursors of short GRBs produced from NS-BH mergers. The timescale of their elementary process is governed by the capture of particles from the NS magnetosphere. Our considerations are markedly different: we do not involve a merger but the newly-formed ν NS-BH binary from a BdHN, still embedded in the HN ejecta which is in our case the supplier of the charged particles needed to establish the elementary process and its associated timescale. In addition, the external magnetic field can reach higher values in view of the strength of the multipole components inferred for the ν NS magnetic field [12, 21] or, if results from the fossil field of the NS which, by induced gravitational collapse, formed the BH. We have shown that these conditions of our system lead to a much energetic (four/five orders of magnitude) process which explains the high-energy emission of long GRBs. Indeed, during the refereeing process of this work, our theoretical prediction on the emission following the elementary process introduced here has found additional experimental support with the detection of TeV emission in GRB 190114C by MAGIC (see R. Ruffini et al. in GCN 23715; <https://gcn.gsfc.nasa.gov/gcn3/23715.gcn3> and Mirzoyan et al. in GCN 2370; <https://gcn.gsfc.nasa.gov/gcn3/23701.gcn3>).

[1] R. Ruffini, J. A. Rueda, M. Muccino, Y. Aimuratov, L. M. Becerra, C. L. Bianco, M. Kovacevic, R. Moradi, F. G. Oliveira, G. B. Pisani, et al., ApJ **832**, 136 (2016), 1602.02732.
 [2] R. Ruffini, J. Rodriguez, M. Muccino, J. A. Rueda,

Y. Aimuratov, U. Barres de Almeida, L. Becerra, C. L. Bianco, C. Cherubini, S. Filippi, et al., ApJ **859**, 30 (2018).
 [3] J. A. Rueda, R. Ruffini, Y. Wang, Y. Aimuratov, U. Barres de Almeida, C. L. Bianco, Y. C. Chen, R. V. Lobato, C. Maia, D. Primorac, et al., JCAP **10**, 006 (2018), 1802.10027.
 [4] C. L. Fryer, J. A. Rueda, and R. Ruffini, ApJ **793**, L36 (2014), 1409.1473.
 [5] C. L. Fryer, F. G. Oliveira, J. A. Rueda, and R. Ruffini, Physical Review Letters **115**, 231102 (2015), 1505.02809.
 [6] L. Becerra, F. Cipolletta, C. L. Fryer, J. A. Rueda, and R. Ruffini, ApJ **812**, 100 (2015), 1505.07580.
 [7] L. Becerra, C. L. Bianco, C. L. Fryer, J. A. Rueda, and R. Ruffini, ApJ **833**, 107 (2016), 1606.02523.
 [8] L. Becerra, M. M. Guzzo, F. Rossi-Torres, J. A. Rueda, R. Ruffini, and J. D. Uribe, ApJ **852**, 120 (2018), 1712.07210.
 [9] L. Becerra, C. L. Ellinger, C. L. Fryer, J. A. Rueda, and R. Ruffini, ArXiv e-prints (2018), 1803.04356.
 [10] R. Ruffini, L. Becerra, C. L. Bianco, Y. C. Chen, M. Karlica, M. Kovačević, J. D. Melon Fuksman, R. Moradi, M. Muccino, G. B. Pisani, et al., ApJ **869**, 151 (2018), 1712.05001.
 [11] R. Ruffini, Y. Wang, Y. Aimuratov, U. Barres de Almeida, L. Becerra, C. L. Bianco, Y. C. Chen, M. Karlica, M. Kovacevic, L. Li, et al., ApJ **852**, 53 (2018), 1704.03821.
 [12] R. Ruffini, M. Karlica, N. Sahakyan, J. A. Rueda, Y. Wang, G. J. Mathews, C. L. Bianco, and M. Muccino, ApJ **869**, 101 (2018), 1712.05000.
 [13] R. Ruffini, R. Moradi, J. A. Rueda, Y. Wang, Y. Aimuratov, L. Becerra, C. L. Bianco, Y.-C. Chen, C. Cherubini, S. Filippi, et al., ArXiv e-prints (2018), 1803.05476.
 [14] D. Christodoulou, Physical Review Letters **25**, 1596 (1970).
 [15] D. Christodoulou and R. Ruffini, Physical Review D **4**, 3552 (1971).
 [16] S. W. Hawking, Physical Review Letters **26**, 1344 (1971).
 [17] S. W. Hawking, Commun. Math. Phys. **25**, 152 (1972).
 [18] A. Papapetrou, Annales de L'Institut Henri Poincare Section (A) Physique Theorique **4**, 83 (1966).
 [19] R. M. Wald, Phys. Rev. **D10**, 1680 (1974).
 [20] G. W. Gibbons, A. H. Mujtaba, and C. N. Pope, ArXiv e-prints (2013), 1301.3927.
 [21] Y. Wang, J. A. Rueda, R. Ruffini, L. Becerra, C. Bianco, and M. Karlica, arXiv e-prints (2018), 1811.05433.
 [22] G. W. Gibbons, A. H. Mujtaba, and C. N. Pope, Classical and Quantum Gravity **30**, 125008 (2013).
 [23] C. W. Misner, K. S. Thorne, and J. A. Wheeler., *Gravitation* (1973).
 [24] R. Ruffini, R. Moradi, J. A. Rueda, L. Becerra, C. L. Bianco, C. Cherubini, S. Filippi, Y. C. Chen, M. Karlica, N. Sahakyan, et al., arXiv e-prints (2018), 1812.00354.
 [25] J. Levin, D. J. D'Orazio, and S. Garcia-Saenz, Physical Review D **98**, 123002 (2018), 1808.07887.